Measuring non-volatile particles properties in the exhaust of an aircraft engine

I.K. Ortega, D. Delhaye, F.X. Ouf, Daniel Ferry, C. Focsa, C. Irimiea, Y. Carpentier, B. Chazallon, P. Parent, C. Laffon, et al.

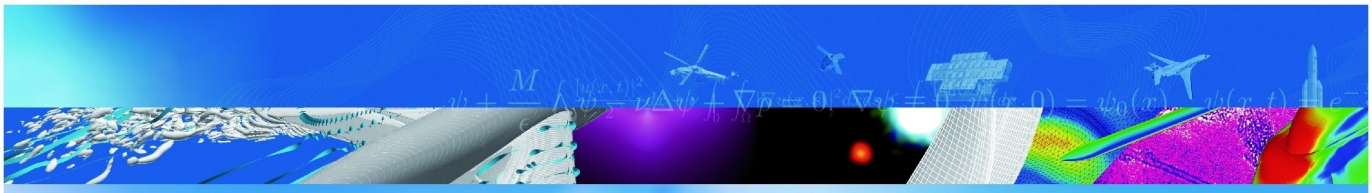

ARTICLE DE REVUE

Measuring non volatile particles properties in the exhaust of an aircraft engine

I. Ortega Colomer (ONERA), D. Delhaye (ONERA),
F.-X. Ouf, D. Ferry, C. Focsa, C. Irimiea, Y. Carpentier,
B. Chazallon, P. Parent, C. Laffon, O. Penanhoat,
N. Harivel, D. Gaffié (ONERA),
X. Vancassel (ONERA)

AEROSPACELAB JOURNAL

No 11, AL11-08, 14 pages

TP 2016-549

70 2016 ans

ONERA

THE FRENCH AEROSPACE LAB

I. K. Ortega, D. Delhaye
(ONERA)

F.-X. Ouf
(Institut de Radioprotection et de Sûreté Nucléaire)

D. Ferry
(Aix-Marseille Université, CNRS, CINaM UMR 7325)

C. Focsa, C. Irimiea, Y. Carpentier, B. Chazallon
(Laboratoire de Physique des Lasers, Atomes et Molécules UMR CNRS 8523, Université de Lille 1 Sciences et Technologies)

P. Parent, C. Laffon
(Aix-Marseille Université, CNRS, CINaM UMR 7325)

O. Penanhoat, N. Harivel
(SNECMA/SAFRAN Group)

D. Gaffié, X. Vancassel
(ONERA)

E-mail : ismael.ortega@onera.fr

DOI : 10.12762/2016.AL11-08

Measuring Non-Volatile Particle Properties in the Exhaust of an Aircraft Engine

The steady growth of air traffic and its foreseen expansion during future years have raised concerns about its potential impact on climate and ground-level air quality. So far, the smoke number has been used to evaluate the non-volatile particulate matter amount emitted by aircraft engines, but it is a poor proxy for modern engine emissions. Therefore, new sampling and measurement techniques have recently been tested on aircraft engine emissions, especially as a new ICAO particle emission standard is currently being developed. Number and mass of emitted particles are generally used, but are not sufficient to fully characterize soot emissions and further address atmospheric impact issues. Chemical composition is crucial to evaluate their atmospheric reactivity. This paper presents a complete set of techniques that have been used to characterize soot emissions from an aircraft engine in a comprehensive manner. It reports results from a campaign on a PowerJet SaM146 engine, performed within the framework of the MERMOSE (*Mesure et Etude de la Réactivité des émissions de MOteurS aEronautiques*) project. It emphasizes the influence of the engine regime, ranging from 30% to 100% of the takeoff thrust, on the various particle properties investigated, including the size, number, morphology and chemical composition.

Introduction

Emissions from aircraft engines include a large variety of gaseous and solid effluents (e.g. [15], [28], [16]). Although these emissions are small compared to other anthropogenic surface emissions (at the present time aviation CO_2 contributes to about 2% to 3% of all anthropogenic sources [21]), they are mostly released in the sensitive region of the upper troposphere and lower stratosphere. In fact, aviation represents a major source of anthropogenic pollution at high altitudes, where background concentrations of these trace substances are low and residence times are long. The unique location of aircraft emissions and the predicted growth of air traffic demand require that particular attention be given to the potential effects of these emissions. One of the key factors regarding aviation environmental impact assessments lies in our ability to accurately characterize aircraft engine emissions, especially soot particles. When emitted at ground level, they may significantly contribute to air quality issues. At typical cruising altitudes, they modify the composition of the atmosphere and hence the Earth's radiative budget, either directly or indirectly, since soot particles may influence contrail formation and subsequently the induced cirrus cloud properties.

Soot particles are sometimes referred to as black carbon (BC), considering their optical and radiative behavior. So far, non-volatile particulate matter (nvPM) emissions, defined as particles present in the engine exhaust at temperatures higher than 350 °C, have been addressed under the ICAO certification process, by using Smoke Number (SN) measurements. These are based on the collection of particles on a filter whose loss of reflectance is analyzed. However, this method has become obsolete and is currently being revised by the CAEP (Committee for Aviation Environmental Protection), for two main reasons. The first reason is that Smoke Number measurements have been developed for old generation engines, with higher levels of soot emissions. The filter collection method can no longer describe the whole size range of the emitted soot particles. In addition, no reliable relationship can be determined between the SN and particle mass or number emission index and it does not provide any information on the size distribution; the SN is therefore a poor proxy to describe nvPM emissions. The second reason is that harmonization is needed between the various transport sector emission measurements. The automobile industry has recently deployed a more suitable measurement protocol, which addresses nvPM properties more specifically, especially the number concentration and mass. As a result, the implementation of an improved and comparable methodology for aviation has become necessary and is described

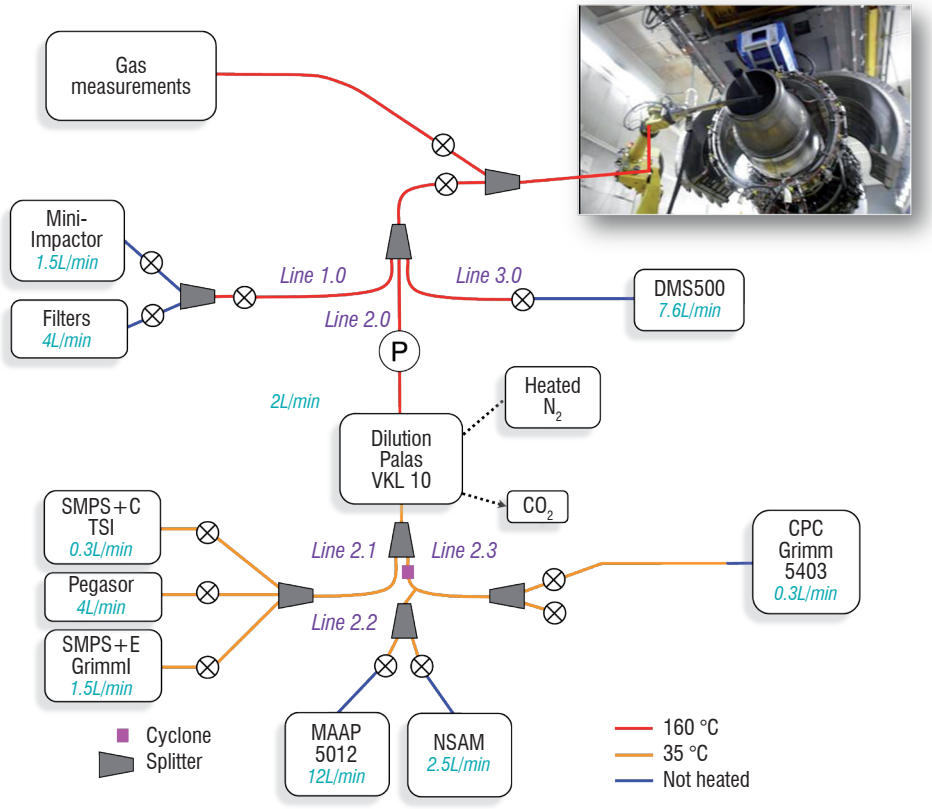

Figure 1 - Schematic diagram of the MERMOSE sampling line

in the AIR6241 (http://standards.sae.org/air6241). This protocol has set the basic methodology for characterizing aircraft engine emitted nvPM for certification purposes. However, such measurements are focused on the particle number and mass. Although these are key parameters to understand the potential environmental impact of aircraft engine emissions, the determination of the chemical composition, and especially the surface chemical composition of emitted particles, is essential to understand the atmospheric reactivity of soot and associated issues more comprehensively.

In this paper we describe a comprehensive experimental set-up to address the characterization of the properties of soot particles emitted by a turbojet engine. In a first section, we describe a typical aircraft exhaust sampling line, used during the MERMOSE project, in order to characterize the soot emitted by a SaM146 engine, its main technical requirements and the engine test plan. In a second part, we focus on the various measurement techniques used, regarding what physical and chemical parameters need to be retrieved and the instrument specific technology involved. Finally, in the last section, we present some results from the MERMOSE engine test campaign.

Experimental set-up

Sampling line

Measuring soot particle properties requires various techniques. For various reasons, the engine exhaust, comprising gaseous combustion products and particles, has to be sampled before being analyzed. The sampling system typically consists of various parts, which are precisely described when used for certification purposes. Generally, sampling is performed in three steps. The exhaust is first sampled by means of a single-hole probe or a rake. It is then transported through a stainless steel line and heated to avoid post-sampling reactions. Finally, the sample reaches the measurement instrument section, to be analyzed. The flow extracted from the probe, measured at atmospheric pressure, was 14 l/min for the gas analysis and 7 l/min for the particle analysis.

Figure 1 depicts the sampling system used to measure gaseous and particulate emissions from a SaM146 jet engine (see Figure 2) during the MERMOSE project.

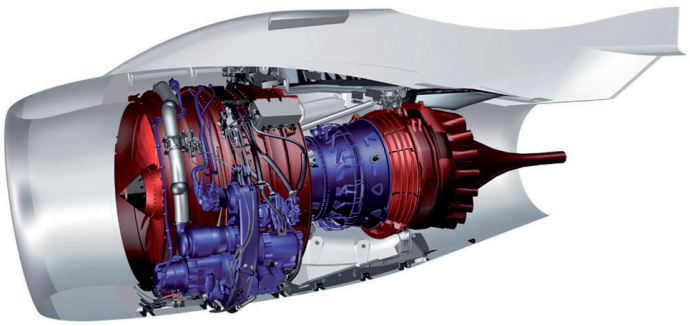

Figure 2 - Powerjet SaM 146 turbofan engine

This sampling line is not fully compliant with the AIR6241 protocol. The main aim of this essay was a complete physicochemical characterization of engine emissions and not certification. For this complete analysis, we used some specific instruments under certain working conditions that made it impossible to fulfill all of the requirements of the AIR6241 protocol. The exhaust was sampled by means of a robotic arm equipped with a single hole probe, located

5 cm away from the exit plane in the primary flow of the engine (tested in an unmixed flow configuration), and moved at various locations to ensure homogeneous sampling. A short section of the transport line after the probe was heated, on demand, in order to prevent vapors from condensing on existing primary particles (formed in the engine) or from nucleating and therefore forming new particles that would modify non-volatile particle measurements. This section was followed by two thermostated 3 m and 5 m lines maintained at 160°C. At the end of these lines, a flow splitter was used to alternately drive the sample to the measuring instruments for the analysis of gases or particles, since these two measurements could not be achieved simultaneously due to the flow rate limitations in the line.

The particle sampling line was divided into 3 thermostated sections:

- The first section was dedicated to particle collection for off-line measurements, (Line 1.0). We used two different collection techniques in parallel. Firstly, a mini impactor [23] to enable the deposition of particles on electron microscopy grids and on silicon windows to perform morphology, structure and chemical composition analyses. Secondly, we used filter samplers, where emitted particles were collected on very high efficiency quartz filters, mainly to measure the elemental to organic carbon ratio, but also to obtain additional data.
- A second separated line (Line 3.0) was equipped with a Fast Aerosol Mobility Size Spectrometer (DMS500) to determine in real time the particle number concentration and size distribution for a size ranging from 5 nm to 1000 nm.
- Finally, a third line (Line 2.0) was used, in which the sampled flow was diluted to decrease the particle concentration, enabling measurements to be made with various instruments and reducing post sampling reactions. It should be noted that the dilution factor obtained with this system was around 10. In addition, we did not use any catalytic stripper, therefore the analyzed PM include both volatile and non-volatile PM. The pressure was measured before the dilution stage using a capacitive absolute manometer thermostated at 200°C. The nitrogen used in the dilution stage was heated at 35°C, since this temperature is the maximum admitted at the instrument inlets. The dilution ratio was determined by measuring the carbon dioxide concentrations, upstream and downstream from the diluter. This ratio was used to correct the particle number measured. The line was split into three subsections to measure particle size distribution, number concentration, soot mass and surface area concentration. Two of the lines were equipped with a stainless steel cyclone (Lines 2.3 and 2.2), used to protect the instruments by cutting off particles larger than 1.69 μm.

Stainless steel lines tend to collect soot and a condensable or semi-volatile coating on their walls while combustion products are transported. No reliable measurement can be obtained during this transient phase, until the inner parts of the line are perfectly coated. The engine was therefore first run at full power for approximately 30 mn, following the AIR6241, and until the measurement instruments provided stable signals. After this line conditioning phase, the engine was operated at various settings, 7%, 30%, 70%, 85% and 100% of the take-off thrust respectively. These settings correspond to the LTO cycle certification regimes (idle, descent, climb-out and take-off) and to a representative regime for cruise conditions (70%). Finally, some post-sampling reactions have to be accounted for when retrieving engine emission indices or initial particle number density. We have done an analysis of the particle loss through the sampling line. We have used a sodium chloride aerosol to measure the penetration factors of the line. We found that these factors were independent of the size of particles. Therefore, they will not affect the shape of the measured size distribution (namely, the count median diameter (CMD) and geometric standard deviation (GSD)). As a consequence, we will consider in this work size distributions without any loss corrections. Without any further details on the influence of pressure and temperature conditions on particle losses, we will also report number, surface and mass concentrations without any correction.

On line measurement techniques

Particle number density

The standard instrument for measuring particle number concentration is the **Condensation Particle Counter** (CPC). In CPC counters, particles are detected and counted by laser scattering in a very similar way to a standard optical particle counter, but in a CPC particles are first grown by condensation to a size of 10-12 μm, enabling the detection of nanoparticles.

The CPC used in the campaigns uses the diffusional thermal cooling method to grow particles to detectable sizes (Figure 3). Using this principle, the CPC used during the campaign was able to measure particles above 5 nm.

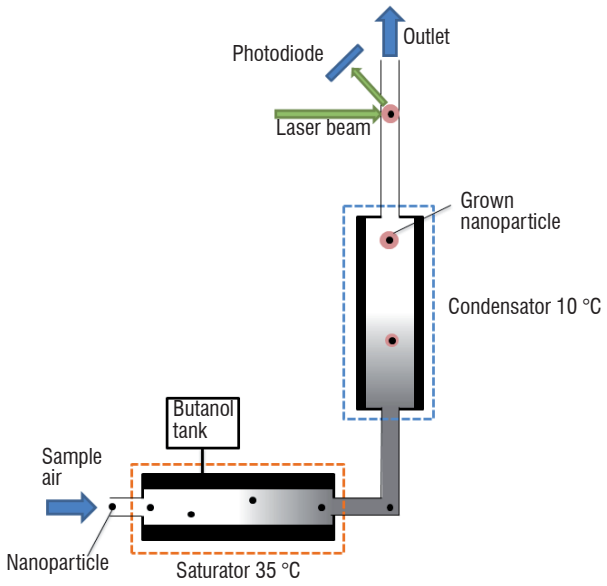

Figure 3 - CPC GRIMM 5.403 schematic diagram

A complementary instrument was used to measure particle number and mass on-line. The **Pegasor Particle Sensor M** (PPS-M) technology is based on the measurement of electrical charges carried by particles. PPS-M (Figure 4) comprises an ejector where the motive fluid flow is generated by pure, particle-free ionized gas. The motive fluid flow generates an under-pressure to the sample inlet and due to the negative pressure gradient, particle-containing gas flows into the sensor. Ionized air and sample flows are mixed, charging the particles in the sample flow very efficiently. Particle charging is linked to the particle size.

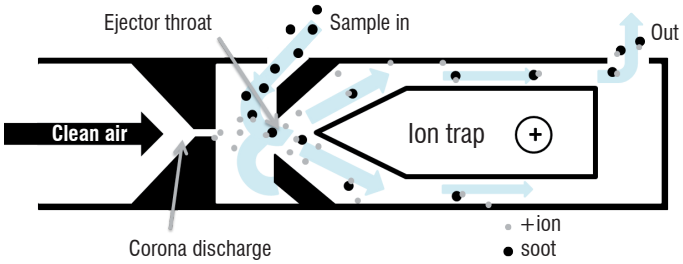

Figure 4 - Schematic representation of PPS-M

Ions that are not attached to the particles are removed from the gas flow by means of an ion trap. When the free ions are removed, the only mechanism carrying electrical current is the flow of charged particles. The electrical current escaping from the sensor with the charged particles can be measured giving a direct, fast, real-time measurement of the particle concentration. The measurement result can be expressed either as mass concentration or as number concentration, or both. With the setting used in the campaign, PPS-M was able to measure particles in the 0.02 – 2.5 μm range.

Particle size distribution measurements

Particle size distribution was measured by means of a **Scanning Mobility Particle Sizer and a Differential Mobility Sizer** DMS500.

- SMPS is based on the principle of the mobility of a charged particle in an electric field. Particles entering the system are neutralized such so that they have a Fuchs equilibrium charge distribution. Then, they enter a Differential Mobility Analyzer (DMA) where the aerosol is classified according to electrical mobility, with only particles of a narrow range of mobility exiting through the output slit. This monodisperse distribution then goes to a CPC, which determines the particle concentration at that size.

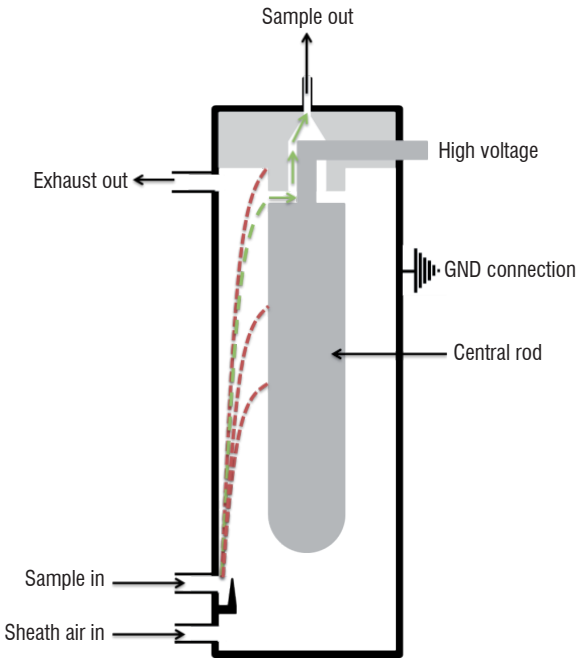

Figure 5 - Schematic representation of a DMA

The DMA (Figure 5) consists of a cylinder with a negatively charged rod at the center; the main flow through the DMA is a particle-free laminar 'sheath' air. The particle flow is injected at the external end of the DMA. Particles with a positive charge move across the sheath flow towards the central rod, at a rate determined by their electrical mobility. Particles of a given mobility exit through the sample slit at the top of the DMA, while all other particles exit with the exhaust flow. The size of the particles exiting through the slit is determined by the charge, the central rod voltage and the flow within the DMA. By exponentially scanning the voltage on the central rod, a full particle size distribution is constructed.

- The DMS500 uses a classifier column (Figure 6) operating at sub-atmospheric pressure. The DMS uses a cyclone that prevents particles larger than 1 μm from entering the instrument. The instrument operates at a fixed pressure of 0.25 bar. This low pressure reduces the residency time, avoiding particle agglomeration [33], helping to isolate the instrument from fluctuating sample pressure and allowing its wide size range (5-1000 nm). The sample gas passes through a corona charger into the classifier column.

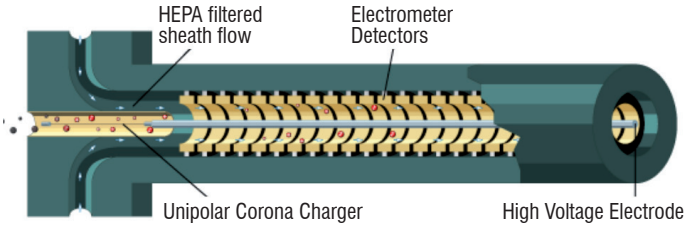

Figure 6 - DMS500 classifier column schematic diagram

The charged aerosol is then introduced into a strong radial electrical field inside a classifier column. This field causes particles to drift through a sheath flow to the electrometer detectors. Particles are detected at various distances down the column, depending on their electrical mobility. The outputs from the electrometers are then processed in real time to provide particle number and size data.

Off line measurement techniques

Black Carbon mass concentration

BC loads were measured using a Thermo Scientific™ 5012 MAAP. This instrument uses a multi-angle absorption photometer to analyze the modification of radiation fields in the forward and back hemisphere of a glass-fiber filter caused by deposited particles.

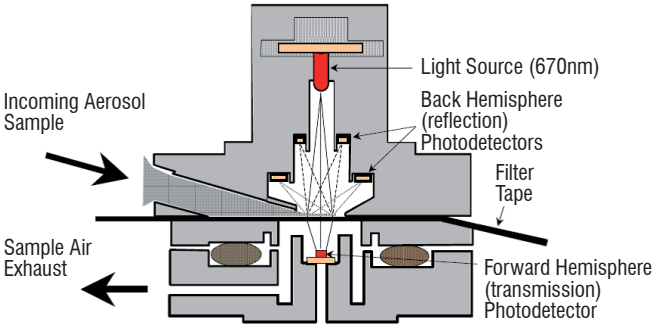

Figure 7 - MAAP detection chamber schematic diagram

The sample flows through the down-tube and is deposited on the glass fiber filter tape. The filter tape will accumulate an aerosol sample towards a threshold value, whereupon the filter tape will automatically advance prior to reaching saturation. Within the detection chamber (Figure 7), a 670 nm visible light source is aimed towards the deposited aerosol and filter tape matrix. The light transmitted into the forward hemisphere and reflected into the back hemisphere is measured by a series of photo-detectors. During sample accumulation, the light beam is attenuated from an initial reference reading from a clean filter spot. The reduction of light transmission, multiple reflection intensities and air sample volume are continuously integrated over the sample run period to provide a real-time data output of black carbon concentration measurements.

Surface area density

The **Nanoparticle Surface Area Monitor** (NSAM) measures the human lung-deposited surface area of particles (reported as $\mu m^2/cm^3$) corresponding to tracheobronchial (TB) and alveolar (A) regions of the lung. The way in which this instrument operates is based on the diffusion charging of sampled particles, followed by the detection of the charged aerosol using an electrometer. The aerosol sample is continuously drawn into the instrument (Figure 8). This flow is split into two flows. One passing through a HEPA filter to produce clean air, which is then ionized using a corona electrode, and the other introduced into the mixing chamber against the current of positive ions produced by corona discharge. The flows are reunited in a mixing chamber, where particles in the aerosol flow mix with the ions carried by the filtered clean air acquiring a positive charge. The separation of particles from direct interaction with the corona needle and/or the strong field near it reduces particle losses and makes the charging process more efficient and reproducible. The charged aerosol then passes through a trap to remove excess ions. The aerosol then moves on to an aerosol electrometer for charge measurement. In the electrometer, current is passed from the particles to a conductive filter and measured by a very sensitive amplifier. The intensity measured is converted in terms of deposited surface in two regions of the respiratory system: tracheobronchial and alveolar.

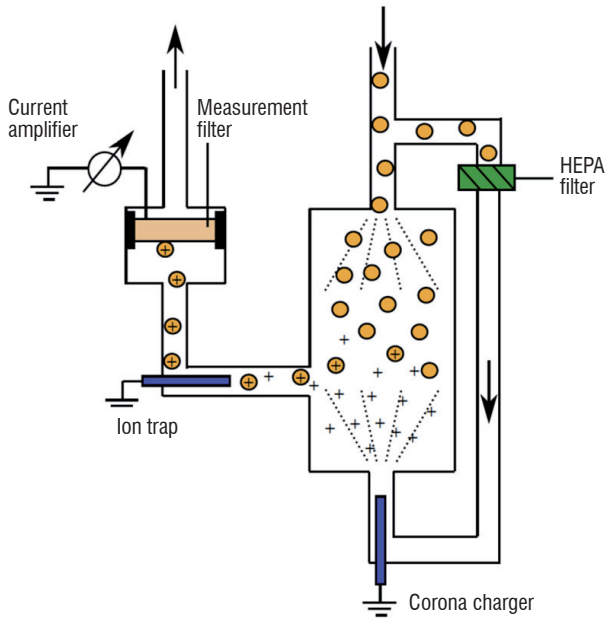

Figure 8 - NSAM 3550 [2] operating principle

The deposited surface area measured by NSAM can be used to determine an active surface equivalent diameter [2].

Morphology and structure characterization

The morphology and structure of the emitted particles were studied by **high-resolution transmission electron microscopy** (HR-TEM), **Raman spectroscopy, near-edge X-ray absorption fine structure spectroscopy** (NEXAFS) and **X-ray photoemission spectroscopy** (XPS).

- **HR-TEM** is an instrument for the high-magnification study of nanomaterials. TEM can simultaneously give information in real space (in the imaging mode) and reciprocal space (in the diffraction mode). The basic principle of TEM is quite similar to their optical counterparts, the optical microscope. The main difference is that TEM uses a focused beam of electrons instead of light to "image" and achieve information about the structure and composition of the sample. An electron gun produces a stream of electrons, which is accelerated towards the sample using a positive electrical potential. This stream is then focused using condenser lenses into a thin, focused, monochromatic beam. The beam strikes the sample and part of it is transmitted through it. This portion of the beam is again focused through objective lenses into an image.
  Samples were studied in both modes (image and diffraction) [25]. Images collected in the imaging mode provide morphological information, as well as the size of primary particles. Those obtained in the diffraction mode provide a more accurate measurement of the carbon layer spacing and enable the determination of the C-C bond lengths.

- **Raman spectroscopy** has been widely used to study various carbonaceous materials, including soot ([30], [31], [4] and references therein). It involves interactions of molecules with the electromagnetic field produced by a laser. The resulting scattered light (Raman scattering) is a radiation type that represents a measure of the vibrational frequency of molecules corresponding to vibrational and/or rotational transitions shifted from the incident laser beam frequency. Soot Raman spectra presents a first order band in the 1000-1700 cm^{-1} region; the complexity of this band varies for different samples and is related to their nature. The G band at 1580 cm^{-1} is solely observed in single crystal graphite. In more complex carbonaceous materials, the D1 and D2 bands appear as the number of defects increases. The D1 band at 1350 cm^{-1} corresponds to a breathing mode of carbon rings [9], which is Raman inactive in the case of perfect infinite graphitic planes. It becomes active and observable in Raman for finite graphene [13]. The D2 band at 1620 cm^{-1} is generally assigned to lattice vibrations analogous to that of the G band, but involving isolated graphene layers, i.e., not directly sandwiched between two other layers [12]. When the carbonaceous material is highly disordered, two further bands D3 and D4 appear. The D3 band at 1500 cm^{-1} is generally very broad and is often assigned to amorphous carbon ([8], [17], [10], [11]). In general, the D4 band is characteristic of highly disordered materials like soot or coal chars ([30], [22], [1], [36], [11]). Its origin is still under debate; some authors assign it to carbon sp^3-sp^2 at the periphery of the crystallites, or to C-C and C=C stretching vibrations in polyene-like structures ([22], [1], [10]).

- **NEXAFS** involves the excitation of electrons from a core level to partially filled and empty states. The decay of core-hole states results in the emission of Auger electrons from valence molecular orbitals (Figure 9), leading to the formation of cascades of secondary electrons in the material, generating a photocurrent proportional to the excitation probability. A NEXAFS spectrum in "total electron yield" mode consists in measuring this photocurrent as a function of the photon energy, in the vicinity of an absorption edge (carbon and oxygen K-edges are of main interest in soot). The peak positions and spectral lineshape in a NEXAFS spectrum are directly related to the nature of these unoccupied electronic states. Given that the photocurrent originates from 5 nanometers from the sample surface, in the case of soot, made up of primary particles of a few nanometers in diameter, this technique can be considered to probe their bulk. A variant of the NEXAFS technique consists in recording the spectra by measuring the Auger electron yield only ("partial electron yield" method),which arises from the 2-3 top-most layers because of their typical low mean free path in matter. Thus, this technique can be both surface and bulk sensitive and is capable of probing both the soot electronic structure and the surface functional groups simultaneously. In the context of carbon-based structures such as soot, NEXAFS measurements can detect specific bonds in molecules (e.g., C=C, C-C, and C-O bonds) [32].

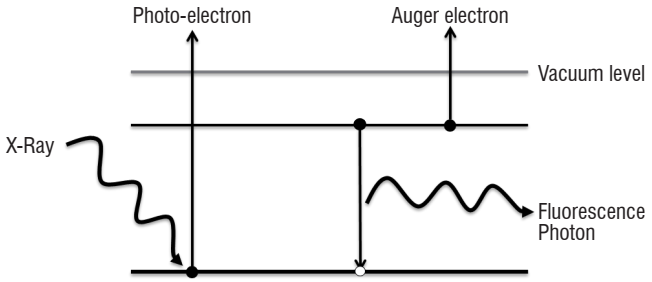

Figure 9 - Energy diagram of the photoabsorption process and the subsequent filling of the core hole by emission of an Auger electron or a fluorescence photon. The Auger electron yield (and excited secondary electron yield) has been used for the NEXAFS spectroscopy of soot.

- **XPS** is another surface characterization technique that can analyze a sample to a depth of 2 to 5 nm. Electrons in specific bound states can be excited by irradiating a sample with x-rays of sufficient energy. A typical XPS experiment uses enough energy to induce the ejection of photoelectrons from the sample (Figure 9) has been used for the NEXAFS spectroscopy of soot. Ejected photoelectrons from core levels have slight energy shifts depending on the outer valence configuration of the material examined. In addition, the specific energy of an elemental core level transition occurs at a specific binding energy that can uniquely identify the element. In a typical XPS spectrum, some of the ejected photoelectrons inelastically scatter through the sample to the surface, while others undergo prompt emission and suffer no energy loss in the process. An electron analyzer measures the kinetic energy of the ejected photoelectrons, producing an energy spectrum of intensity (number of photoelectrons versus time) versus binding energy (the energy that the electrons had before they left the atom). Each energy peak in the spectrum corresponds to a specific element. In addition to identifying elements in the sample, the peak area is proportional to the number of atoms present in each element. The sample chemical composition is obtained by calculating the respective contribution of each peak area.

Chemical composition characterization

Energy-dispersive X-Ray spectroscopy (EDX), **Organic to Elemental Carbon ratio** (OC/EC) analysis, **Laser Two-Step Mass Spectrometry** (L2MS) and **Time-of-Flight Secondary Ion Mass Spectrometry** (ToF-SIMS) techniques were also used for a complete chemical characterization of the samples.

- EDX spectroscopy uses a beam of electrons or high-energy radiation to excite core electrons to high energy states, creating a low-energy vacancy in the atom electronic structures. This leads to a cascade of electrons from higher energy levels until the atom regains a minimum-energy state. Due to energy conservation, the electrons emit X-rays during their transition to lower energy states. It is these X-rays that are being measured in X-ray spectroscopy. Since each element has a different nuclear charge, the energies of the core shells and, more importantly, the spacing between them vary from one element to the next. While not every peak in the spectrum of an element is exclusive to that element, there are enough characteristic peaks to be able to determine the composition of the sample, given sufficient resolving power.

- The OC/EC ratio was analyzed using Thermal-Optical Analysis fully compliant with the IMPROVE protocol [7]. First, the sample is heated in a completely oxygen-free helium atmosphere in four increasing temperature steps to remove all organic carbon from the sample. The transition from the third temperature to the fourth (from 500°C - 700°C) quickly decomposes inorganic carbonates, producing a sharp, characteristic peak. It should be noted that only one filter was used for the sampling, thus organic vapors can be adsorbed on the filter, leading to an overestimation of OC/TC. Samples collected at 30% engine regime are more sensible to this bias, since the organic compound concentration in the exhaust is higher in this regime.

- L2MS and ToF-SIMS are two mass spectrometry techniques able to measure the surface chemical composition of aerosol particles. In L2MS [14] (Figure 10), the adsorbed phase is probed by nanosecond laser desorption and then the ejected molecules are ionized with a second nanosecond laser and further

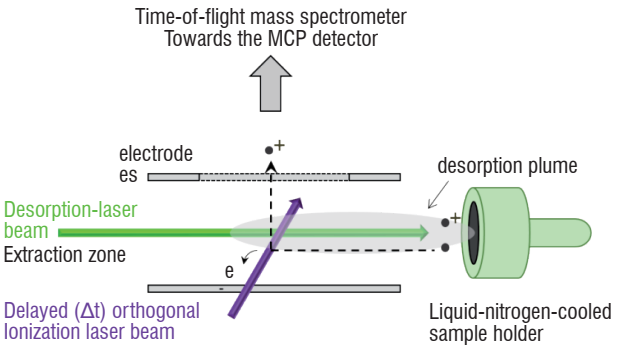

Figure 10 - L2MS technique schematic diagram

mass-separated by ToF-MS. For desorption, the collimated beam of a nano-second Nd:YAG laser is directed through a circular pinhole onto the sample. The laser irradiance can be carefully controlled to maximize the signal of the parent molecules and to avoid the direct fragmentation of the species during the desorption step. This configuration is particularly well suited for the detection of aromatic species like Polycyclic Aromatic Hydrocarbons (PAHs).

- ToF-SIMS is similar to L2MS. It uses a pulsed primary ion beam (Bi_3^+) to desorb and ionize species from a sample surface. The resulting secondary ions are accelerated into a mass spectrometer, where they are mass analyzed by measuring their time-of-flight from the sample surface to the detector (Figure 11). In addition to the mass spectra acquired from the molecular species on the sample surface, this instrument is able to provide an image of the sampled surface, enabling the distribution of individual species to be visualized on the surface of the sample. There are three different modes of analysis in TOF-SIMS:

The main advantage of the L2MS technique compared to ToF-SIMS is the low fragmentation of the analyzed compounds achieved through a careful tuning of desorption and ionization energies (Figure 12, left panel). On the one hand, the highest mass resolution achieved in L2MS is around 1000 while in ToF-SIMS, depending of the substrate morphology, it is possible to reach up to 10000. As can be seen in Figure 12, right panel, the L2MS mass resolution is not sufficient to distinguish different compounds with the same integer mass but different elemental composition, as opposed to ToF-SIMS.

Results

Particle number, mass, surface area and size distribution

The properties of non-volatile emitted particles vary with the engine thrust rate. The size distribution, the particle number density, the mass and the surface concentration can be affected.

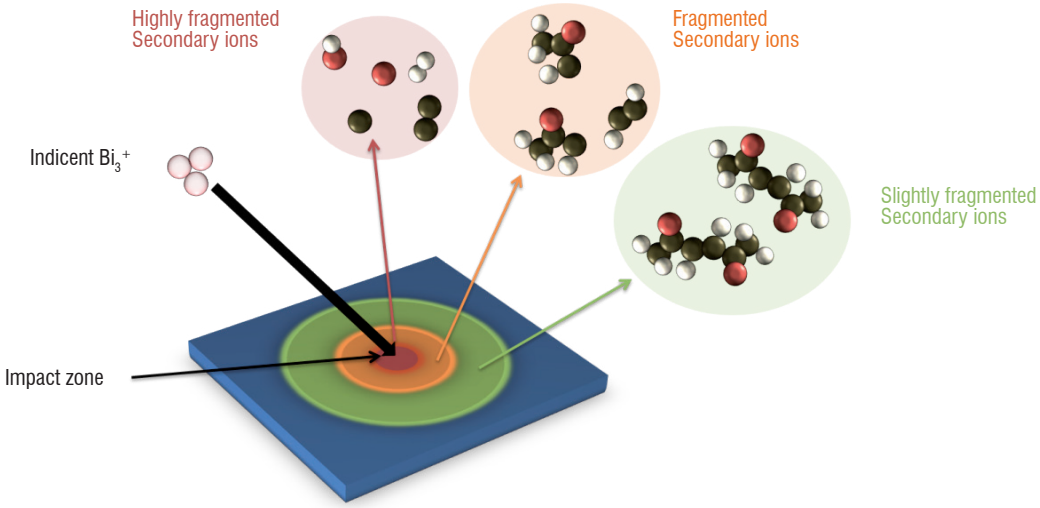

Figure 11 - Ion beam desorption/ionization performed in the ToF-SIMS instrument

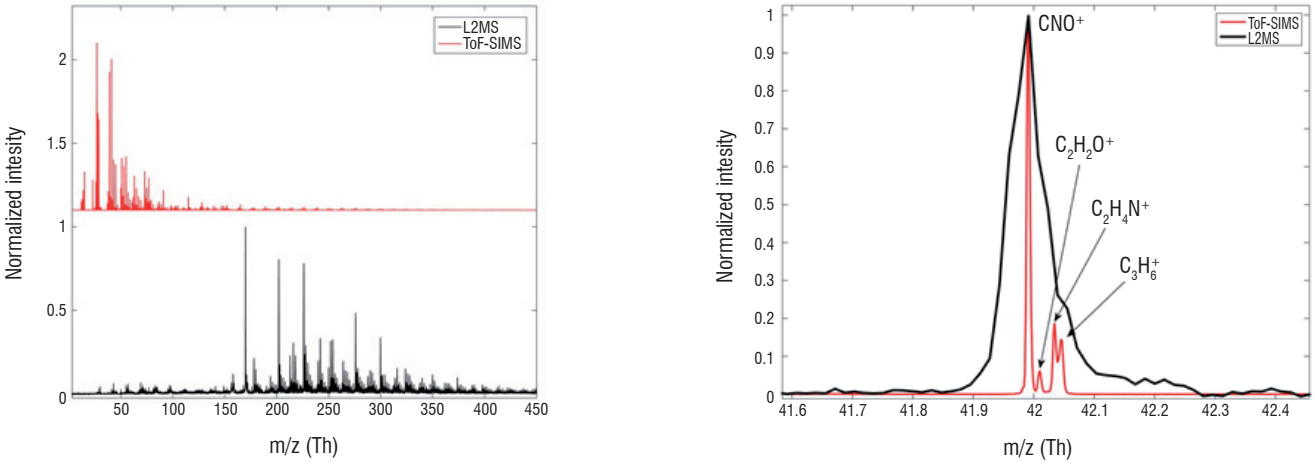

Figure 12 - L2MS and ToF SIMS spectra obtained from the same soot sample collected at 70% engine regime. Left panel, illustration of fragmentation produced in L2MS and ToF-SIMS techniques. Right panel, illustration of the different mass resolution obtained with L2MS and ToF-SIMS for the same sample.

For all of the investigated engine regimes, a monomodal log-normal type particle size distribution has been obtained (Figure 13). The modal diameter has also been found to grow with increasing regime up to 85% (Figure 14) and to remain constant beyond. The greatest change is produced between the 30% case regime, where the modal diameter is 24.1+/- 1.2 nm, and the 70% regime, where the modal diameter increases up to 47.2 +/- 2.6 nm. The studies by [5] on a C-130 Hercules and by [6] on various military turbofan, turboprop and turboshaft aircraft also showed a trend of increasing particle diameter with increasing engine power settings. On the other hand, the results reported from the APEX campaign showed that the particle diameter first decreases when the engine thrust increases from low to medium settings and then increases at higher thrust [19].

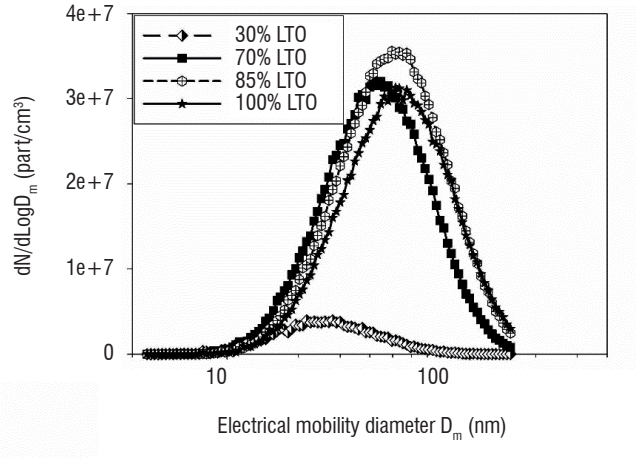

Figure 13 - Size distributions for number concentration obtained for various engine regimes (values not corrected for particle loss in the sampling line)

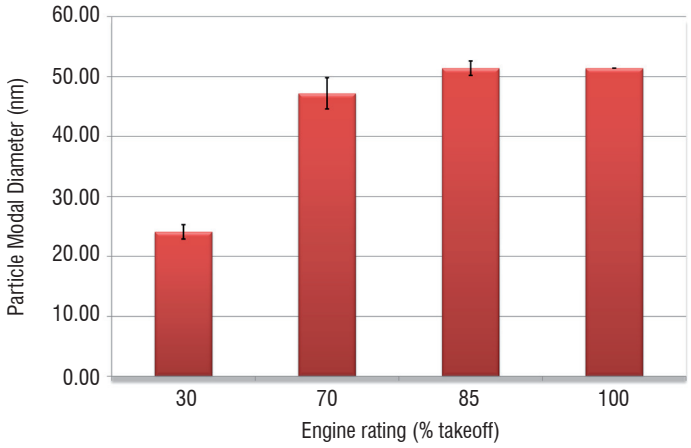

Figure 14 - Particle modal diameter for each engine regime

Number and mass concentrations present similar trends, both increase with the engine regime up to 85%, remaining almost constant between 85% and 100%. In general, CPC and PPS-M agreement on particle number is quite good, with the only exception of the 30% regime, where the particle number density measured by CPC is larger than that measured by PPS-M. The reason behind this discrepancy might be the different nature of the particles produced at 30%, which include a larger fraction of organic particles, probably volatile, that are measured by the CPC but not measured by the PPS-M. In addition, the cutoff diameter for both instruments was different; while CPC counted particles larger than 5 nm, the PPS-M cutoff was 20 nm. Since the size distribution for the 30% regime is shifted towards smaller sizes, this difference might be more evident in this regime. Again the largest shift is observed between the 30% and 70% regimes. These results

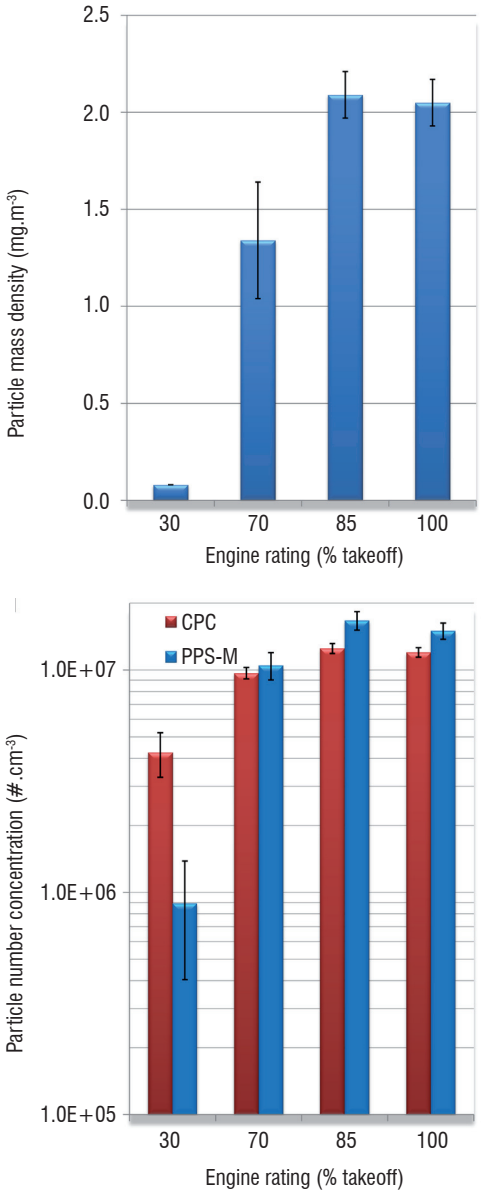

Figure 15 - Top: Particle mass measured for each engine regime
Bottom: Particle number measured for each engine regime

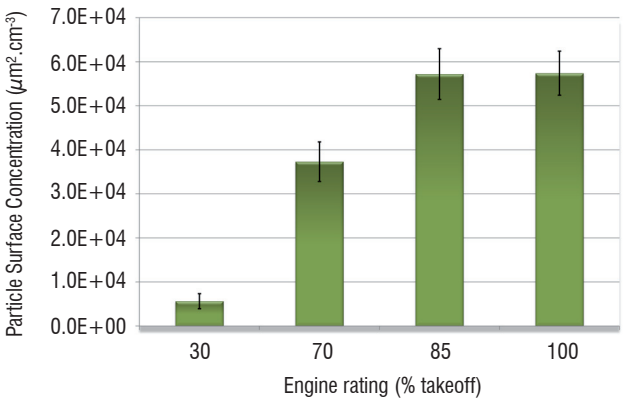

Figure 16 - Particle surface concentration for each engine regime

are in line with those presented by previous studies, where in most of the cases an increase in the engine regime results in an increase in the particle emission index ([28], [19], [6], [3]).

The surface concentration evolves in a similar way regarding the other investigated parameters. We found a large increase in surface concentration when the engine regime increased from 30% to 70% and an almost constant value between 85% and 100%. The values obtained range from roughly 6 x 10^3 to 6 x 10^4 $\mu m^2.cm^{-3}$. The studies reporting the surface concentration of airplane engine emitted particles are scarce. [29] measured the surface concentration of particles emitted from a GE-J85-5L in the NASA Lewis Research Center using an altitude-simulation facility at 95% and 100% engine regime, for various simulated altitudes. The authors reported a slight increase in the surface concentration between 95 and 100% at 36,000 ft. However, no difference could be observed at 41,000 and 45,000 ft. In addition, the authors highlighted a large impact of the simulated altitude on the particle surface concentration, increasing with decreasing altitude. Results ranged from 5.87 x 10^3 $\mu m^2.cm^{-3}$ at 45,000 ft to 1.28 x 10^4 $\mu m^2.cm^{-3}$ for measurements at 5,000 ft. [28] reports a 2 x 10^5 $\mu m^2.cm^{-3}$ surface concentration of particles emitted by ATTAS aircraft in flight (26,000 ft) with an engine regime of about 30%. Discrepancies can originate from different sampling or testing conditions (ground level, altitude test cell, in flight) but also from the different engine technologies used. The GE-J85-5L and the ATTAS engine (RR-SNECMA M-45H) are old generation engines from the 60s and 70s whereas the SaM146 has been certified very recently.

Morphology and structure characterization results

HR-TEM images illustrate the turbostratic structure of soot aggregates (Figure 17, top right panel) where a few graphene carbonaceous layers having a small lateral extension are stacked, with a random rotation angle between them, forming basic structural units concentrically oriented in space to form an onion-like structure [26].

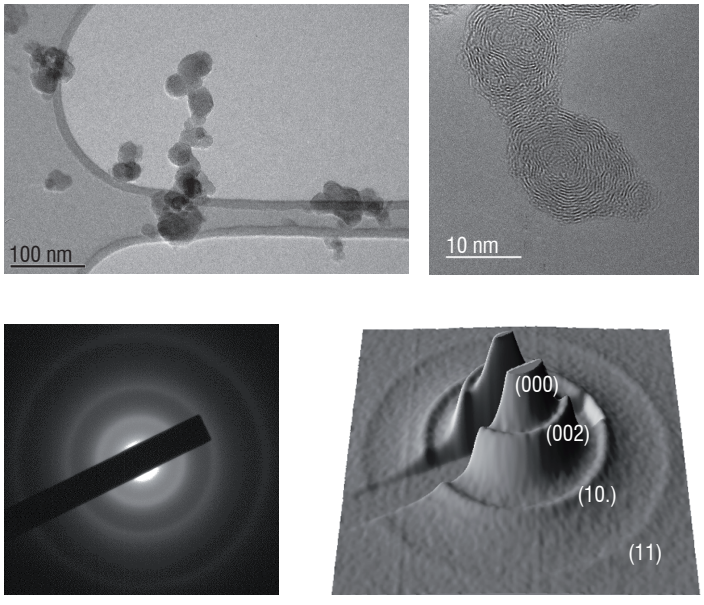

Figure 17 - Top left panel: HR-TEM image showing soot aggregates. Top right panel: Soot primary particles presenting a turbostratic structure. Bottom left panel: Diffractogram showing concentric rings. Bottom right panel: 3D representation of the diffractogram with diffraction ring indices

The morphology of the samples obtained at various engine regimes has been found to be very similar [25]. Carbon bonding lengths ranged from 0.138 to 0.141nm, which is slightly shorter than in graphite ($l_{C\text{-}C}$ = 0.142 nm) as usually determined for atmospheric soot [20]. The geometric length of carbonaceous layers ranged from 2.54 to 3.66 nm for engine thrust levels between 30%-100%. These values are of the same order of magnitude but higher than those reported by [34] for a CFM-56-2 engine (~0.7 nm).

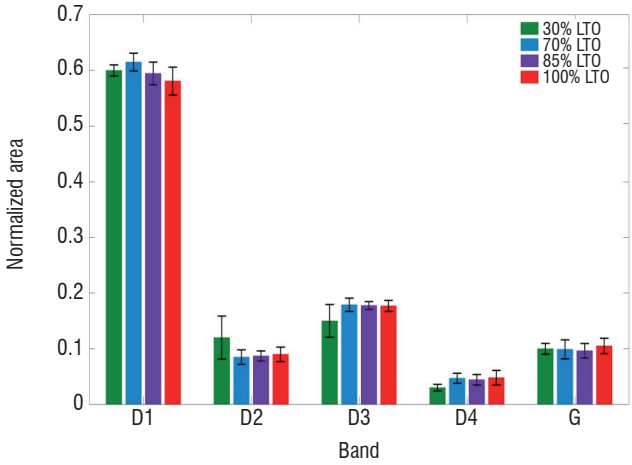

Figure 18 - Normalized area for D1, D2, D3, D4 and G bands for each sample analyzed

Analyzed samples presented very similar Raman spectra regardless of the engine regime [25] (Figure 18). The intensity of the fitted bands pointed to crystalline domains between 2.67 and 3.06 nm, in good agreement with the HR-TEM results. Also, the relative intensities of the D1 and D2 bands corresponded to a highly defective graphite structure. The presence of a D4 band indicated the presence of non-graphitic carbon, though it presented a rather low intensity.

As in the case of Raman and HR-TEM, the NEXAFS and XPS measurements did not show remarkable differences between the samples collected at different engine regimes [25]. With regard to the structure of the soot particles found in the samples, NEXAFS showed that their surface consists mainly of graphene layers of the same size as in the bulk, although more defective. The surface also presented a high concentration of unsaturated organic hydrocarbons that were not detected in the bulk. XPS spectra showed that the soot particles were poorly oxidized, with a slight enhancement of the oxidation rate at the very surface. Oxide functions were essentially ketones and carbonyls, with few hydroxyls and quinones.

Chemical composition characterization results

EDX analyses performed in the samples collected during the SAM146 campaign revealed that particles are free of metallic elements (within the detection limit of the technique) and are systematically made up of carbon, oxygen and traces of sulfur [25], due to its presence in the fuel. In addition, we found that the elemental bulk chemical composition did not evolve with engine thrust. Thus, on average, the elemental chemical composition of the samples can be considered as ~97% of carbon, ~3% of oxygen and atomic traces of sulfur (~0.1%).

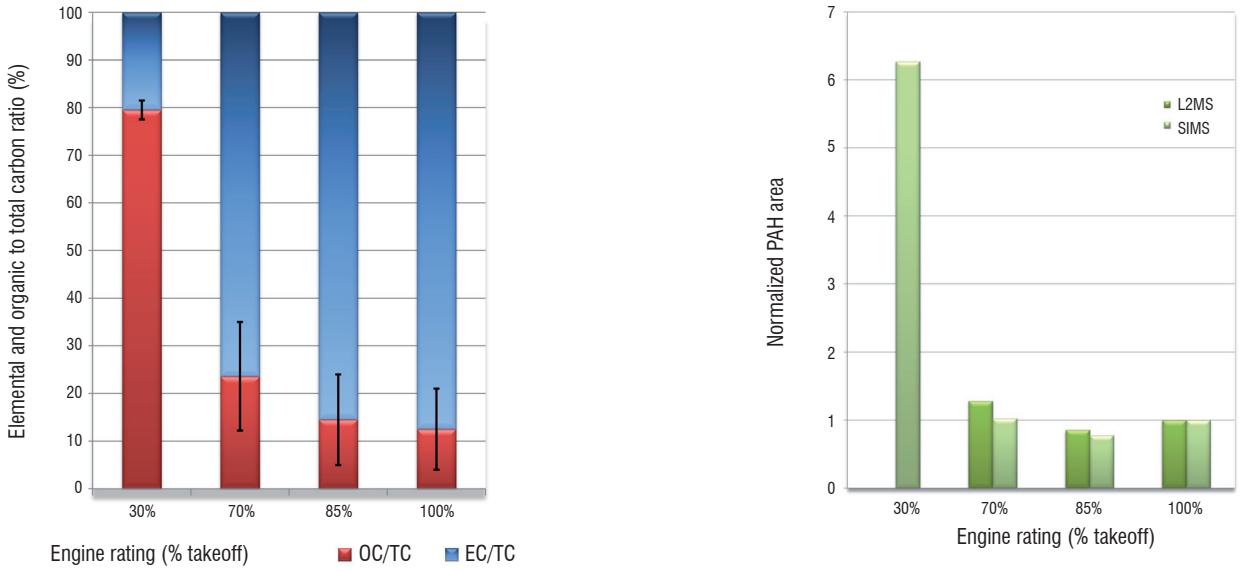

Figure 19 - Left panel: Organic carbon (red) and elemental carbon (blue) content of various samples analyzed
Right panel: Total PAHs content of various samples analyzed by the TOF-SIMS (light green) and L2MS (dark green) technique

Figure 19 (left panel) shows the OC/EC ratios measured for the samples collected during the SAM146 campaign at various engine regimes. We can see how the organic content decreases as the engine thrust increases, with a large decrease from ~79% for the 30% regime to ~24% for the 70% engine regime. In addition, L2MS and ToF-SIMS were used to determine the PAH content of various samples (Figure 19, right panel). As can be seen, both techniques present a good agreement with regard to the total PAH content. Unfortunately, we could not measure the total PAH content of the 30% sample with L2MS due to the low load of the sample. The total PAH content found by these two techniques is also in good agreement with the organic carbon content found in the OC/EC analysis. These results were in line with those reported in the literature, where the OC/EC ratio was found to decrease when the engine regime increased ([27]).Nevertheless, in the results reported by [27], the amount of organic carbon drops between the 7% and 30% engine regimes, with just a slight drop between the 30% and 80% regimes. In our case, the main drop in the organic content is observed between the 30% and 70% regimes. One possible reason for these differences might be the overestimation of the OC/TC ratio for the 30% regime due to the absorption of organic compounds present in the gas phase in the filters.

ToF-SIMS showed the presence on molybdenum oxides in some of the samples. These species were heterogeneously distributed over the sample surface. To obtain a better insight of the origin of these compounds, we performed an imaging study of the samples. Thanks to this, we were able to distinguish two different kinds of aerosol particles, containing sulfate and molybdenum oxides respectively, from the substrate (Silicon wafer) (Figure 20).

We found that the particles containing sulfate were smaller and were distributed over all of the substrate, while the signal corresponding to molybdenum oxides was associated with lubricant oil droplets collected on the substrate. Most probably, these compounds come

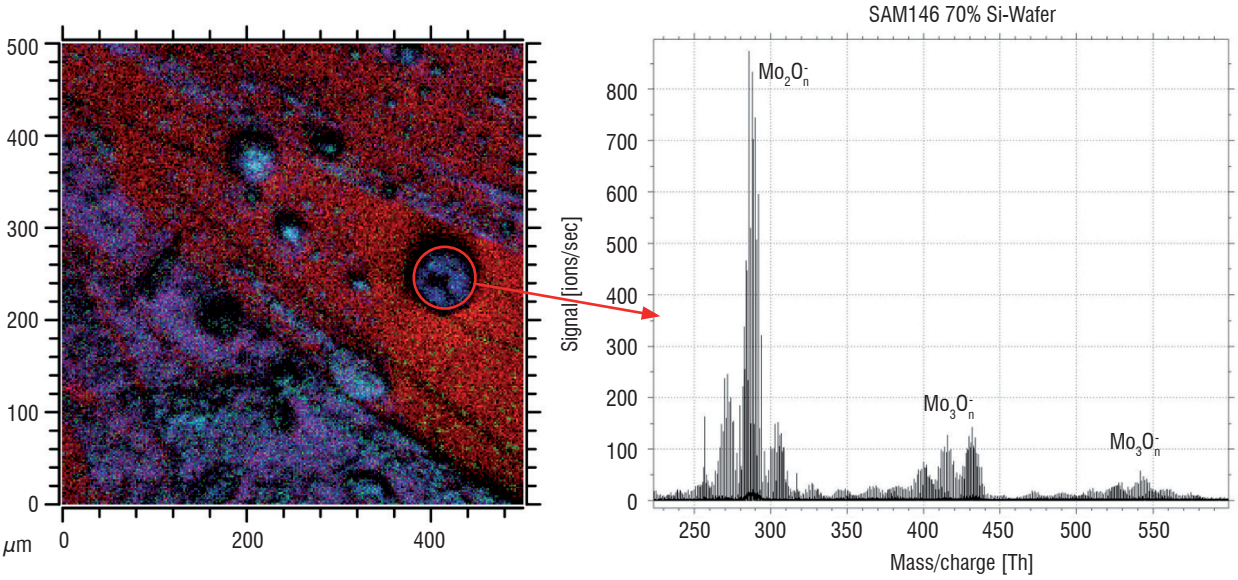

Figure 20 - Left panel: Mapping of an aerosol sample collected over a silicon wafer; the red areas indicate the presence of SiO_2^- ions, the blue areas indicate the presence of $Mo_2O_6^-$ ions and the green areas indicate the presence of HSO_4^- ions. Right panel: mass spectra of the selected particle showing Molybdenum oxide peaks.

from the motor gear, in which molybdenum doped stainless steel is used for some parts. The presence of oil droplets on the engine exhaust has also been reported in previous studies. A study from [35] identified lubricant oil droplets in the particulate matter emissions from various commercial aircraft at two airports.

Conclusions

In this work we presented a complete sampling and characterization methodology of nVPM. We applied it to the measurement of the nvPM emitted by a SaM146 engine. It was operated at various engine regimes corresponding to four LTO cycle certification regimes and a regime representative of a cruise fuel air ratio condition. We found that the size, number, mass and surface concentration of the emitted particles increase when the engine regime increases up to 85%, staying constant above this limit. The largest increase for all of these properties was found between the 30% and 70% engine regimes. These results are in line with those available in the literature. From the point of view of chemical characterization, the three different techniques used point to a larger content of organic carbon in the 30% sample. L2MS and ToF-SIMS show a high content in PAHs in this sample as well. In this case, though previous results show a similar trend, the organic content found in the 30% sample is greater than that reported in previous studies. Regarding the physical and chemical properties of the emitted soot primary particles, we did not find a significant change between the various engine regimes. These particles present an onion-like nanostructure, consisting of concentric graphitic layers with small lateral extensions ranging from 2.54 to 3.66 nm. They present a low degree of oxidation, with a slight enhancement at the surface. Our results show how some properties, like the morphology of soot particles, were not affected by the engine regime, while others like the chemical composition or particle size, number mass and surface concentration were largely affected. These results illustrate the importance of a complete characterization of nvPM emissions to fully evaluate the potential impact of emissions on climate ■

Acknowledgements

This work was supported by the CORAC MERMOSE project for the characterization of emissions by aircraft engines and funded by the DGAC (French Civil Aviation Authority).

References

[1] E. BAR-ZIV, A. ZAIDA, P. SALATINO, O. SENNECA - *Diagnostics of Carbon Gasification by Raman Microprobe Spectroscopy*. Proceedings of the Combustion Institute, 28, 2369–2374, 2000.

[2] S. BAU - *Étude des moyens de mesure de la surface des aérosols ultrafins pour l'évaluation de l'exposition individuelle*. Thèse de Doctorat de l'INPL, Nancy, 3 Décembre 2008.

[3] J. CAIN, M.J. DEWITT, D. BLUNCK, E. CORPORAN, R. STRIEBICH, D. ANNEKEN, C. KLINGSHIRN, W.M. ROQUEMORE,R. VANDER WAL - *Characterization of Gaseous and Particulate Emissions from a Turboshaft Engine Burning Conventional, Alternative, and Surrogate Fuels*. Energy and Fuels, 27, 2290-2302, 2013.

[4] T. CATELANI, G. PRATESI, M. ZOPPI - *Raman Characterization of Ambient Airborne Soot and Associated Mineral Phases*. Aerosol Science & Technology, 48, 13–21, 2014.

[5] M. D. CHENG, E. CORPORAN, M. J. DEWITT, C. W. SPICER, M. W. HOLDREN, K. A. COWEN, A. LASKIN, D. B. HARRIS, R. C. SHORES, R. KAGANN, R. HASHMONAY - *Probing Emissions of Military Cargo Aircraft: Description of a Joint Field Measurement Strategic Environmental Research and Development Program*. Journal of the Air and Waste Management Association, 58, 787-796, 2008.

[6] M. D. CHENG, E. CORPORAN - *A Study of Extractive and Remote-Sensing Sampling and Measurement of Emissions from Military Aircraft Engines*. Atmospheric Environment, 44, 4867-4878, 2010.

[7] J. C. CHOW, J. G. WATSON, L.-W. A. CHEN, M. C. O. CHANG, N. F. ROBINSON, D. TRIMBLE, S.KOHL - *The IMPROVE_A Temperature Protocol for Thermal/Optical Carbon Analysis: Maintaining Consistency with a Long-Term Database*. Journal of the Air & Waste Management Association, 57, 1014-1023, 2007.

[8] A. CUESTA, P. DHAMELINCOURT, J. LAUREYNS, A. MARTINEZ-ALONSO, J. M. D. TASCON - *Raman Microprobe Studies on Carbon Materials*. Carbon, 32, 1523–32, 1994.

[9] E. DI DONATO, T. TOMMASINI, G. FUSTELLA, L. BRAMBILLA, C. CASTIGLIONI, G. ZERBI, C. D. SIMPSON, K. MULLEN, F. NEGRI - *Wavelength-Dependent Raman Activity of D2h Symmetry Polycyclic Aromatic Hydrocarbons in the D-Band and Acoustic Phonon Regions*. Chemical Physics, 301, 81-93, 2004.

[10] B. DIPPEL, H. JANDER, J. HEINTZENBERG - *NIR FT Raman Spectroscopic Study of Flame Soot*. Physical Chemistry Chemical Physics, 1, 4707–4712, 1999

[11] B. DIPPEL, J. HEINTZENBERG - *Soot Characterization in Atmospheric Particles from Different Sources by NIR FT Raman Spectroscopy*. Journal of Aerosol Science, 30 (Suppl.1), 907–908, 1999.

[12] M. S. DRESSELHAUS, G. DRESSELHAUS, Topics in applied physics, vol. 51. Berlin: Springer-Verlag, p. 3-57, 1982.

[13] A. ECKMAN, A. FELTEN, A. MISCHENKO, L. BRITNELL, R. KRUPKE, K. S. NOVOSELOV, C. CASIRAGHI - *Probing the Nature of Defects in Graphene by Raman Spectroscopy*. Nano Letters, 12, 3925-3930, 2012.

[14] A. FACCINETTO, P. DESGROUX, M. ZISKIND, E. THERSSEN, C. FOCSA - *High-Sensitivity Detection of Polycyclic Aromatic Hydrocarbons Adsorbed onto Soot Particles Using Laser Desorption/Laser Ionization/Time-of-Flight Mass Spectrometry: An Approach to Studying the Soot Inception Process in Low-Pressure Flames*. Combustion and Flame, 158, 227-239, 2011.

[15] D. J. HOFMANN, J. M. ROSEN - *Balloon Observations of a Particle Layer Injected by Stratospheric Aircraft at 23 km*. Geophysical Research Letters, Vol. 5(6), 1978

[16] J.E.PENNER, D.H. LISTER, D.J. GRIGGS, D.J. DOKKEN, M. MCFARLAND (Eds.) – *Intergovernmental Panel on Climate Change (IPCC)*. Aviation and the Global Atmosphere Special Report, Cambridge University Press, UK., pp 373, 1999

[17] T. JAWHARI, A. ROID, J. CASADO - *Raman Spectroscopic Characterization of some Commercially Available Carbon Black Materials*. Carbon, 33, 1561–1565, 1995.

[18] G. KATAGIRI, H. ISHIDA, A. ISHITANI - *Raman Spectra of Graphite Edge Planes*. Carbon, 26, 565–571, 1998.

[19] J. S. KINSEY, Y. DONG, D. C. WILLIAMS, R. LOGAN - *Physical Characterization of the Fine Particle Emissions from Commercial Aircraft Engines During the Aircraft Particle Emissions eXperiment (APEX) 1-3*. Atmospheric Environment, 44, 2147-2156, 2010.

[20] V. KOVACS KIS, M. POSFAI, J. L. LABAR - *Nanostructure of Atmospheric Soot Particles*. Atmospheric Environment, 40, 5533−5542, 2006.

[21] D. S. LEE, G. PITARI, V. GREWE, K. GIERENS, J. E. PENNER, A. PETZOLD, M. J. PRATHER, U. SCHUMANN, A. BAIS, T. BERNTSEN, D. IACHETTI, L. L. LIM, R. SAUSEN - *Transport Impacts on Atmosphere and Climate: Aviation*. Atmospheric Environment, 44, 4678-4734, 2010.

[22] T. LIVNEH, E. BAR-ZIV, P. SALATINO, O. SENNECA - *Evolution of Reactivity of Highly Porous Chars from Raman Microscopy*. Combustion Science and Technology, 153, 65–82, 2000.

[23] D. LOTTIN, D. FERRY, J.-M. GAY AND D. DELHAYE - *Towards an Identification of Aircraft Soot among Urban Background: Focus on Nanoparticles Emitted by CFM56 Turbofan Engines*. European Aerosol Conference, Granada, Spain, 2 - 7 September 2012.

[24] F.-X. OUF, E. BRUGIÈRE, D. FERRY, S. PONTREAU AND J. YON - *Characterization of Aerosols Produced by a Commercial Combustion Aerosol Generator MiniCASTTM 5201: EC/TC, Size Distribution, Morphology and Optical Properties*. European Aerosol Conference, Granada, Spain, 2-7 September 2012.

[25] P. PARENT, C. LAFFON, I. MARHABA, D. FERRY, T.Z. REGIER, I.K. ORTEGA, B. CHAZALLON, Y. CARPENTIER, C. FOCSA - *Nanoscale Characterization of Aircraft Soot: A HRTEM, Raman, NEXAFS and XPS Study*. Carbon, under review, 2015.

[26] M. PAWLITA, J. N. ROUZAUD, S. DUBER - *Raman Microspectroscopy Characterization of Carbon Blacks: Spectral Analysis and Structural Information*. Carbon, 84, 479−490, 2015.

[27] A. PETZOLD, F.P. SCHRÖDER - *Jet Engine Exhaust Aerosol Characterization*. Aerosol Science and Technology, 28, 63-77, 1998.

[28] A. PETZOLD, J. STROM, F.P. SCHRODER, B. KARCHER, *Carbonaceous Aerosol in Jet Engine Exhaust: Emission Characteristics and Implications for Heterogeneous Chemical Reactions*. Atmospheric Environment, Vol. 33(17), 2689–2698, 1999.

[29] J. E. RICKEY - *The Effect of Altitude Conditions on the Particle Emissions of a J85-GE-5L Turbojet Engine*. NASA Technical Memorandum TM-106669, 52p, 1995.

[30] A. SADEZKY, H. MUCKENHUBER, H. GROTHE, R. NIESSNER, U.PÖSCHL - *Raman Microspectroscopy of Soot and Related Carbonaceous Materials: Spectral Analysis and Structural Information*. Carbon, 43, 1731-42, 2005.

[31] J. SCHMID, B. GROB, R. NEISSNER, P. IVLEVA - *Multi-Wavelength Raman Microscopy for Rapid Prediction of Soot Oxidation Reactivity*. Analytical Chemistry, 83, 1173-1179, 2010.

[32] J. STOHR, *NEXAFS Spectroscopy*. Springer, Berlin, 1992.

[33] J. P. R. SYMONDS, K. REAVELL - *Calibration of a Differential Mobility Spectrometer*. European Aerosol Conference, Salzburg, Austria, September 9-14, 2007.

[34] R. L.VANDER WAL, V. M. BRYG, C. H. HUANG - *Aircraft Engine Particulate Matter: Macro- Micro- and Nanostructure by HRTEM and Chemistry by XPS.* Combustion and Flame, 161, 602-611, 2014.

[35] Z. YU, S.C. HERNDON, L.D. ZIEMBA, M.T. TIMKO, D.S. LISCINSKY, B.E. ANDERSON, R.C. MIAKE-LYE - *Identification of Lubrication Oil in the Particulate Matter Emissions from Engine Exhaust of In-Service Commercial Aircraft*. Environmental Science and Technology, 46, 9630 -9637, 2012.

[36] V. ZAIDA, E. BAR-ZIV, L. R. ZADOVIC, Y.-J. LEE - *Further Development of Raman Microprobe Spectroscopy for Characterization of Char Reactivity*. Proceedings of the Combustion Institute, 31, 1873–1880, 2006.

List of acronyms

BC	(Black Carbon)
CAEP	(Committee for Aviation Environmental Protection)
CPC	(Condensation Particle Counter)
DMA	(Differential Mobility Analyzer)
DMS	(Differential Mobility Sizer)
EDX	(Energy-Dispersive X-Ray Spectroscopy)
HEPA	(High Efficiency Particulate Air Filter)
HR-TEM	(High Resolution Transmission Electron Microscopy)
ICAO	(International Civil Aviation Organization)
L2MS	(Laser Two-Step Mass Spectrometry)
MAAP	(Multi-Angle Absorption Photometer)
MERMOSE	(Mesure et Etude de la Réactivité des Emissions de Moteurs Aéronautiques)
NEXAFS	(Near-Edge X-Ray Absorption Fine Structure)
NSAM	(Nanoparticle Surface Area Monitor)
nvPM	(Non-Volatile Particulate Matter)
PAH	(Polycyclic Aromatic Hydrocarbons)
PPS-M	(Pegasor Particle Sizer M-Sensor)
SMPS	(Scanning Mobility Particle Sizer)
SN	(Smoke Number)
TEM	(Transmission Electron Microscopy)
ToF-SIMS	(Time-of-Flight Secondary Ion Mass Spectrometry)
XPS	(X-Ray Photoelectron Spectroscopy)

Ismael Ortega received his PhD degree in atmospheric Sciences in 2006 from the University of Jaén and the Spanish national council for research (CSIC). From 2007 to 2013 He has worked as post-doc researcher in the Atmospheric Science division of the University of Helsinki and in the Department of Environmental Science and Analytical Chemistry at the University of Stockholm. During this period, he focused his research in the field of atmospheric aerosol, more specifically in understanding the formation of aerosol particles in the atmosphere. In 2013 he joins the Laboratoire de Physique des Lasers, Atomes et Molécules PhLAM at University of Lille 1, where we focused his work in the characterization airplane engine emission. From November 2015 he is member of the department of Fundamental and applied Energetics (DEFA) at ONERA, where he keeps working on airplane engine emission characterization.

David Delhaye (PhD University of Marseille, 2007) has been working as an emission measurement specialist at ONERA since 2004. He received in 2007 the Jean Bricard award for his PhD dealing with the characterization of aircraft engine soot. He then joined the DLR in 2008 at the Institute of Atmospheric Physics (DLR Oberpfaffenhofen - Germany) in framework of European Network of Excellence ECATS scientific exchange for 15 months where he worked on various national or European research projects (BIOCLEAN, CONCERT, SAMPLE). He has been working since 2009 in the ONERA's Atmospheric Environment team with a special emphasis on soot particles characterization. He has been involved in EU projects like ECATS (NoE, 2005-2010), SAMPLE1&2&3 (EASA, 2009-2011) and also national funded projects like MERMOSE (2012-2015). He is a member of the SAE–E31 experts subcommittee on aircraft engine particulate matter emissions.

François-Xavier Ouf is a research scientist at IRSN (Institut de Radioprotection et de Sûreté Nucléaire). He joined in 2002 the Aerosol Physics and Metrology Laboratory and received the degree of Doctor of Physics from the University of Rouen in 2006. He received the same year the Jean Bricard award for his PhD dealing with the characterization of fire generated aerosols. Since 2006 he is in charge of researches and studies dealing with the physico-chemical characterization of combustion generated aerosol and their impact on the containment of nuclear installations (radioactive release, HEPA filters clogging). He is involved in many industrial and academic partnerships and since 2010 he is chairing the working group "combustion aerosols" of the EAA. He is the author or co-author of more than 25 publications in high-impact international journals.

Daniel Ferry is a research scientist at the Centre National de la Recherche Scientifique (CNRS) in Marseille, France. He received his PhD degree in Material Sciences in 1997 from the University Aix-Marseille. During 10 years he studied interactions of molecules with solid surfaces and the structure, dynamics and thermodynamics of molecular layers. Since 2006 his research aims at understanding physical and chemical properties of carbonaceous aerosols. He is currently working at determining the link between nanoscopic properties of solid aerosols and their reactivity with atmospheric gases by using electron microscopy as well as photonic spectroscopies.

Cristian Focsa (43) received his PhD in molecular spectroscopy in 1999 from the University of Lille 1. After a post-doc in University of Waterloo (Canada), he was appointed as Associate Professor (1999) and then Professor (2009) at University of Lille 1. Since 2002 he is the leader of the ANATRAC (Analysis of Traces) research group (currently 9 people) within the Laboratoire de Physique des Lasers, Atomes et Molécules (PhLAM, UMR CNRS 8523). Since 2010 he is the director of CERLA (Centre d'Etudes et de Recherches Lasers et Applications). His main current research interest is in the applications of laser ablation in environment, medicine, and materials sciences.

Cornelia Irimiea received the M.S. degree in Plasma Physics, Spectroscopy and Self-Organization from "Alexandru Ioan Cuza University", Iasi, Romania, in 2011. She is currently pursuing a Ph.D degree at Lille 1 University, Villeneuve d'Ascq, France. Her current research interests include the study of soot mechanisms formation in laboratory flames using laser based techniques coupled with mass spectrometry.

Yvain Carpentier received his PhD degree in 2009 from the University Paris XI. His PhD thesis was focused on the production and spectroscopic characterization of astrophysically-relevant carbonaceous molecules and nanograins. Since 2011, he is Associate Professor of Physics at the PhLAM Laboratory (University Lille 1). He works in particular on the L2MS technique to determine the surface chemical composition of aerosols, especially soot particles.

Bertrand Chazallon received his Ph.D. degree from University of Lyon1 in 1999 on the spectroscopy, neutron diffraction and molecular modeling of gas hydrates. He joined the PhLAM laboratory of University Lille 1 in 2001 as associate professor to work on multiphasic processes of environmental interests. Since 2012, Dr. Chazallon is Professor in Physics at the University of Lille1. His current research is focused on the ice nucleation activity of anthropogenic and biogenic aerosols. He develops original methods for CO_2 capture and mitigation of greenhouse gases by hydrate crystallization.

Philippe Parent is Directeur de Recherche at the Centre National de la Recherche Scientifique, France. He received the degree of Doctor in Physics (Material Sciences) in 1991 at the Université Pierre-et-Marie Curie, Paris, France. During 15 years of research at LURE, the first synchrotron radiation facility in France (Orsay), he contributed to the development of soft X-ray absorption spectroscopy applied to surface science and environmental physical chemistry. In 2005 he moved to Paris (Laboratoire de Chimie-Physique, Matière et Rayonnement) and then in 2013 to Marseille (Centre Interdisciplinaire de Nanoscience), where he presently works on the surface properties of nanoscale materials, with emphasis on environmental solids, using spectroscopic tools (laboratory and synchrotron) and nanoscience techniques.

Carine Laffon is a research scientist at the CNRS (Centre National de la Recherche Scientifique), France. She received the degree of Doctor of Physics from the Université de Paris Sud (Orsay) in 1990. Her research interest initially focused on the structure and electronic properties of solids, of adsorbates on metal surfaces, and of molecular solids using X-ray absorption spectroscopy. She is currently working at the Centre Interdisciplinaire de Nanoscience de Marseille (CINaM) on the nanostructure, reactivity and electronic properties of aerosols and environmental solids, using electronic spectroscopies with laboratory and synchrotron light sources (NEXAFS, photoemission).

Olivier Penanhoat became engineer from Ecole Centrale de Lyon in 1986, and received his PhD in theoretical mechanics from University Pierre et Marie Curie in 1990. He has been working at Snecma for more than 20 years, mainly in the field of combustion (technology, CFD, pollution, future fuels). He was involved in many European programs, in particular as coordinator of LOWNOX III and LOPOCOTEP technological projects. Currently he is coordinator of the European network FORUM-AE, dedicated to all environmental issues linked to aircrafts emissions and is Snecma representative to the emissions technical group of the ICAO Committee on Aviation Environmental Protection. He was also formerly responsible of SaM146 engine certification and was till 2016 professor of combustion in Mines de Nancy.

Nadine Harivel received her Ph.D. degree in 1981 from University of Poitiers. She joined Snecma in 1981 where she was involved in combustor studies. She is currently in charge of measurement of aircraft engine exhaust gas concentrations, smoke number and particulate matter. She is involved in the emission certification tests of civil engines.

Daniel Gaffié obtained his PhD from the University Paul Sabatier of Toulouse in 1982 in the field of modelling and numerical simulation of the rheology of multiphase dispersed flows. Second PhD on the numerical simulation of hyperbolic systems encountered in Mechanics Fluid applications. From 1997 to 2009, he leads research unit on “Multiphase Turbulent combustion modeling”. Since 2010, he helds at ONERA the position of Special Advisor on Aeronautical Propulsion systems providing expert technical assistance in R&D for the aeronautical applications. Alongside, Daniel Gaffié ensures since 1989, a teaching charge at the University Pierre et Marie Curie in the framework of the master "Energy and Environment" and assumes a charge of Professor at the Superior Engineer School for Aeronautic Techniques and Car Manufacturing.

Xavier Vancassel received a PhD degree in chemical physics from the University of Strasbourg, 2003. He joined ONERA in 2006, after a two years post-doctoral research position at the University of Oxford. He currently heads the Engine Emission and Environmental impact research unit, in the Fundamental and Applied Energetics Department. He has been working on aviation emissions related projects since 2000 and has been involved in many international and national programmes.

Office National d'Études et de Recherches Aérospatiales
Chemin de la Hunière et des Joncherettes – BP 80100
91123 PALAISEAU Cedex
Tél. : +33 1 80 38 60 60 - Fax : +33 1 80 38 65 10
http://www.onera.fr